Translational Oncology
www.transonc.com

Volume 12 Number 7 July 2019 pp. 879–888 879

Preclinical Evaluation of the Acute Radiotoxicity of the α-Emitting Molecular-Targeted Therapeutic Agent ^{211}At-MABG for the Treatment of Malignant Pheochromocytoma in Normal Mice

Hitomi Sudo[*], Atsushi B. Tsuji[*], Aya Sugyo[*], Kotaro Nagatsu[†], Katsuyuki Minegishi[†], Noriko S. Ishioka[‡], Hiroshi Ito[§], Keiichiro Yoshinaga[*] and Tatsuya Higashi[*]

[*]Department of Molecular Imaging and Theranostics, National Institute of Radiological Sciences, National Institutes for Quantum and Radiological Science and Technology (QST-NIRS), Inage, Chiba 263-8555, Japan; [†]Department of Radiopharmaceuticals, National Institute of Radiological Sciences, National Institutes for Quantum and Radiological Science and Technology (QST-NIRS), Inage, Chiba 263-8555, Japan; [‡]Department of Radiation-Applied Biology Research, Quantum Beam Science Research Directorate, National Institutes for Quantum and Radiological Science and Technology, Takasaki, Japan; [§]Department of Radiology and Nuclear Medicine, Fukushima Medical University, 1 Hikariga-oka, Fukushima 960-1295, Japan

Abstract

The α-emitter ^{211}At-labeled *meta*-astatobenzylguanidine (^{211}At-MABG) has a strong antitumor effect on pheochromocytoma xenograft tumors and holds great promise as a new therapeutic option for malignant pheochromocytoma. To evaluate the acute radiation-related toxicity of ^{211}At-MABG, we conducted biodistribution and dosimetry studies of ^{211}At-MABG in ICR mice to estimate the doses absorbed by organs. We determined the maximum tolerated doses (MTD) of ^{211}At-MABG on the basis of body weight loss and assessed the acute radiation-related toxicity induced by MTD administration on the basis of organ weights, histologic features, hematologic indices, and biochemical indices. The biodistribution and dosimetry studies of α-emitting ^{211}At-MABG revealed high doses absorbed by most organs except the brain in ICR mice. The administration of 1.1, 2.2, and 3.3 MBq of ^{211}At-MABG induced transient body weight loss, and 4.4 MBq of ^{211}At-MABG induced unrecoverable body weight loss; thus, the MTD was 3.3 MBq for ICR mice. Although by day 5 the administration of 3.3 MBq had induced some radiation-related toxicity symptoms—such as body weight loss and leucopenia, which are generally observed in radiation therapy including β^--emitting radiopharmaceuticals—the mice had recovered by day 28. We observed no unexpected severe toxicity in ICR mice despite the high absorbed doses in most organs, especially the thyroid, heart, stomach, and adrenal glands. Our findings suggest that therapeutic treatments with appropriate doses of ^{211}At-MABG estimated by dosimetry in each patient could be tolerated, although lower doses may initially be necessary to ensure patient safety in the first-in-human study.

Translational Oncology (2019) 12, 879–888

Introduction

Pheochromocytoma is a neuroendocrine tumor arising from the adrenal glands [1]. Although most pheochromocytomas are benign, approximately 10% result in systemic metastasis [1–3]. The tumor mass and secreted catecholamine induce several pathologic conditions associated with mortality [1,4,5]. The treatment options for patients with malignant pheochromocytoma are limited and include chemotherapy with cyclophosphamide, vincristine, and dacarbazine [6,7], and

Address all correspondence to: Atsushi B. Tsuji or Keiichiro Yoshinaga, Department of Molecular Imaging and Theranostics, National Institute of Radiological Sciences, National Institutes for Quantum and Radiological Science and Technology (QST-NIRS), 4-9-1 Anagawa, Inage, Chiba 263-8555, Japan.
E-mail: tsuji.atsushi@qst.go.jp
Received 12 March 2019; Revised 3 April 2019; Accepted 10 April 2019

1936-5233/19
https://doi.org/10.1016/j.tranon.2019.04.008

molecular-targeted radionuclide therapy with the norepinephrine analog *N*-benzylguanidine radiolabeled with a β^--emitter ^{131}I (*meta*-^{131}I-iodobenzylguanidine, ^{131}I-MIBG). Chemotherapy with cyclophosphamide, vincristine, and dacarbazine has a limited duration of effects and confers no survival benefits [6,8], whereas ^{131}I-MIBG prolongs survival [8]. Even with high-dose ^{131}I-MIBG, however, long-term survival is limited [9]. Therefore, more effective therapies are required.

Compared with β^--emitters, α-emitters have higher energy deposition, resulting in higher cytotoxic effects to cells [10]. The α-emitter ^{211}At belongs to the halogen family, and like ^{131}I and *meta*-iodobenzylguanidine, it can be used to radiolabel *meta*-astatobenzylguanidine, forming *meta*-^{211}At-astato-benzylguanidine (^{211}At-MABG) [11]. *In vitro* and *in vivo* evaluations by Vaidyanathan et al. revealed that ^{211}At-MABG has biologic properties similar to those of ^{131}I-MIBG [11]. We previously demonstrated strong antitumor effects of ^{211}At-MABG in nude mice bearing pheochromocytoma xenograft tumors, suggesting potential efficacy of ^{211}At-MABG as a new therapeutic option for malignant pheochromocytoma [12].

In general, preliminary preclinical studies must be performed to evaluate radiation-induced and ligand-induced toxicity in animals to support first-in-human studies of new therapeutic radiopharmaceuticals for oncology [13]. Radiation-induced toxicity is generally evaluated on the basis of dosimetry in animals and knowledge of radiation-induced toxicity in humans [13]. If possible, dosimetry in human is more informative than that in animals because the biodistribution of radiotracers in animals is not completely consistent with that in humans but similar [14–16]. Unfortunately, ^{211}At-MABG is not appropriate for imaging; however, the distribution of ^{211}At-MABG is almost consistent with that of radioiodine-labeled MIBG in mice [11,17]. Therefore, surrogate imaging probes such as ^{123}I-MIBG and ^{131}I-MIBG would be appropriate for dosimetry in patients. Accumulating documentation of clinical experiences with ^{131}I-MIBG therapy [6,18] indicates that the radioiodine-labeled MIBG distribution may vary among patients. Thus, the best way to determine the therapeutic dose of ^{211}At-MABG in the first-in-human study would be to perform dosimetry of radioiodine-labeled MIBG in each patient. In some cases, however, unexpected radiation-related toxicity was induced by α-emitting radiopharmaceuticals; for example, two patients receiving ^{225}Ac-PSMA-617 developed grade 2 xerostomia [19]. Therefore, it is important to evaluate whether ^{211}At-MABG induces unexpected radiation-related toxicity before performing first-in-human studies.

In the present study, we first conducted a biodistribution study of ^{211}At-MABG in ICR mice to estimate the doses absorbed by normal organs. We additionally determined the maximum tolerated dose (MTD) of ^{211}At-MABG for ICR mice on the basis of body weight loss and assessed the acute radiotoxicity induced by MTD on the basis of organ weights, histologic features, hematologic indices, and biochemical indices.

Materials and Methods

Production of ^{211}At and Radiosynthesis of ^{211}At-MABG

The radionuclide ^{211}At was produced by irradiation of a Bi target (New Metals and Chemicals, Essex, UK) with an external vertical beam and an NIRS AVF-930 cyclotron (Sumitomo Heavy Industries, Tokyo, Japan) with recovery through dry distillation, as described previously [20]. The ^{211}At-MABG was radiosynthesized under no-carrier-added conditions through radiohalogenation of *meta*-trimethylsilylbenzylguanidine (ABX Advanced Biochemical Compounds, Radeberg, Germany) with *N*-chlorosuccinimide (Tokyo Chemical Industries, Tokyo, Japan) in trifluoroacetic acid (Tokyo Chemical Industries, Tokyo, Japan), as described previously [11]. Unpurified ^{211}At-MABG was trapped on a tC18 cartridge (Sep-Pak light; Waters, Milford, MA), washed with 1 ml of pure water (Fujifilm Wako Pure Chemical), and then eluted as the final product with 2 ml of 5% EtOH. The radiochemical yield was 57.8% ± 7.6% (decay-uncorrected), and the radiochemical purity was greater than 98.8%.

Animals

The animal experimental protocol was approved by the Animal Care and Use Committee of the National Institute of Radiological Sciences, and all animal experiments were conducted in accordance with the National Institute of Radiological Sciences Institutional Guidelines Regarding Animal Care and Handling. Male ICR mice (6 weeks old) were obtained from CLEA Japan (Tokyo, Japan). Pelleted food (Funabashi Farm, Chiba, Japan) and water were provided *ad libitum*. The animal room had a controlled temperature (23°C ± 3°C), humidity (50% ± 20%), and light-dark cycle (12 hours on and 12 hours off).

Biodistribution of ^{211}At-MABG

Male ICR mice (n = 5 per time-point) received 185 kBq of ^{211}At-MABG in 100 μl phosphate-buffered saline (PBS) *via* the tail vein. The mice were euthanized by isoflurane inhalation at 1.5 minutes, 1 hour, 3 hours, and 24 hours after ^{211}At-MABG administration. The blood and organs were dissected and weighed, and radioactivity was measured with a γ-counter (ARC-7001, Aloka, Tokyo, Japan). Uptake in organs and tissues, except for the thyroid, is represented as the percentage injected radioactivity dose per gram (% ID/g), and thyroid uptake is represented as % ID because the thyroid is very small. As previously described [21,22], the mean absorbed dose per unit injected activity of ^{211}At-MABG was estimated with the area under the curve on the basis of the biodistribution data and the mean energy emitted per transition of ^{211}At (4×10^{-13} Gy kg/Bq s) and a daughter nuclide ^{211}Po (1.2×10^{-12} Gy kg/Bq s) with a correction for the branching ratio [23]. In addition, a radiation weighting factor of 5 was used, as recommended by the Medical Internal Radiation Dose (MIRD) Committee [24]. The estimated absorbed dose is expressed as Sv/MBq.

Body Weight Measurements

Mice (body weight, 30.1 ± 1.6 g) were intravenously administered ^{211}At-MABG (1.1, 2.2, 3.3, and 4.4 MBq; n = 4 or 5 per dose) or PBS (n = 4). The body weights were measured at least twice per week for 28 days after administration. When the body weight was more than 20% below that at day 0 or signs of a moribund state were observed, the mouse was euthanized humanely by isoflurane inhalation.

Organ Weight Measurement; Histologic, Hematologic, and Biochemical Analyses

In a separate experiment, mice (body weight, 30.8 ± 2.7 g) were intravenously administered 3.3 MBq of ^{211}At-MABG (n = 3) or PBS (n = 3). Whole organs (brain, thyroid, heart, lungs, liver, spleen, pancreas, stomach, intestine, kidneys, adrenal glands, and left femur) were resected and weighed 5 and 28 days after administration. For histologic analysis, the organs were fixed in 10% neutral-buffered formalin and embedded in paraffin. The organ sections (1 μm thick)

were deparaffinized and stained with hematoxylin and eosin. The images were obtained with a NanoZoomer S60 virtual slide scanner (Hamamatsu Photonics, Shizuoka, Japan). For hematologic analysis, blood was collected *via* the tail vein at days 5 and 28, and the red blood cells, white blood cells, platelets, hemoglobin, and hematocrit were immediately analyzed with a Celltac Alpha hematology analyzer (Nihon Kohden, Tokyo, Japan). For biochemical analysis of triiodothyronine (T3), thyroxine (T4), epinephrine, and norepinephrine, blood was collected from the cardiac ventricle at days 5 and 28. Plasma was separated from the blood and stored at −80°C. T3 and T4 concentrations were measured with the mouse T3 ELISA and mouse T4 ELISA kits (NOVUS Biologicals, Littleton, CO). Epinephrine and norepinephrine concentrations were measured with an epinephrine/norepinephrine ELISA kit (Abnova, Taipei, Taiwan).

Statistical Analysis

All statistical analyses were conducted in GraphPad Prism 7 software (GraphPad Software, San Diego, CA). Comparison of body weight between day 0 and the other days was conducted with repeated-measures one-way analysis of variance with Dunnett's multiple-comparison test. Other data were analyzed with two-tailed unpaired Student's *t* test. $P < .05$ was considered statistically significant in all experiments.

Results

Biodistribution of ^{211}At-MABG

Although high radioactivity of ^{211}At-MABG in the blood (16.9% ID/g) was observed 1.5 minutes after administration, the radioactivity rapidly decreased to 2.3% ID/g at 1 hour and 0.5% ID/g at 24 hours (Table 1). High uptake at 1.5 minutes after injection was also observed in the heart, lungs, kidneys, and adrenal glands, and the uptake decreased over time, similar to that in the blood, except in the adrenals, where the uptake of 18.0% ID/g at 1.5 minutes decreased to 10.2% ID/g at 1 hour, but the uptake was maintained at approximately 10% ID/g until the end of the 24-hour observation period (Table 1). The uptake in most other organs decreased over time, although the uptake in the stomach and intestine increased from 1.5 minutes to 1 hour (Table 1). The uptake in the intestine was relatively low (maximum, 6.4% ID/g at 1 hour), whereas that in the stomach was relatively high (maximum, 12.9% ID/g at 1 hour; Table 1).

Table 1. Biodistribution of ^{211}At-MABG in ICR Mice

(% ID/g)	1.5 Minutes	1 Hour	3 Hours	24 Hours
Blood	16.9 ± 2.5	2.3 ± 0.3	2.0 ± 0.4	0.5 ± 0.1
Brain	1.3 ± 0.2	0.3 ± 0.0	0.2 ± 0.0	0.1 ± 0.0
Heart	26.8 ± 4.5	11.5 ± 1.5	9.3 ± 1.1	2.0 ± 0.4
Lung	37.5 ± 6.4	10.2 ± 2.0	7.3 ± 0.1	1.9 ± 0.5
Liver	5.8 ± 1.2	7.2 ± 0.7	4.8 ± 1.0	0.8 ± 0.1
Spleen	2.8 ± 1.2	7.5 ± 0.6	6.4 ± 0.6	2.0 ± 0.5
Pancreas	7.1 ± 1.6	4.5 ± 0.5	3.1 ± 0.3	0.7 ± 0.0
Stomach	3.4 ± 1.2	12.9 ± 3.3	12.8 ± 2.8	4.5 ± 1.3
Intestine	5.0 ± 1.6	6.4 ± 0.9	5.5 ± 0.5	1.4 ± 0.3
Kidney	19.6 ± 7.6	5.6 ± 2.0	3.5 ± 0.5	1.1 ± 0.2
Adrenal gland	18.0 ± 2.9	10.2 ± 0.7	10.0 ± 2.5	10.8 ± 5.2
Muscle	3.7 ± 0.5	1.8 ± 0.1	1.5 ± 0.3	0.4 ± 0.0
Bone	3.6 ± 0.2	2.4 ± 0.2	2.0 ± 0.3	0.5 ± 0.2
(% ID)	1.5 Minutes	1 Hour	3 Hours	24 Hours
Thyroid	0.3 ± 0.1	0.4 ± 0.1	0.5 ± 0.1	0.3 ± 0.1

Data are expressed as the percentage of injected radioactivity dose per gram (% ID/g), except the thyroid, which is expressed as injected radioactivity dose (% ID). Data are expressed as the mean ± standard deviation.

Table 2. Estimated Absorbed Dose* of ^{211}At-MABG

Organ	Absorbed Dose (Sv/MBq)	Absorbed Dose (Sv/3.3 MBq)
Brain	0.6	2.2
Heart	22.2	73.2
Lung	19.5	64.3
Liver	10.9	36.1
Spleen	13.8	45.6
Pancreas	7.4	24.5
Stomach	26.8	88.6
Intestine	12.0	39.7
Kidney	9.7	32.0
Adrenal gland	24.0	79.3
Muscle	3.6	11.9
Bone	4.6	15.1
Thyroid	25.0	82.4

* The radiation weighting factor of 5 was used for the estimation.

Dosimetry of ^{211}At-MABG

Because ^{211}At is an α-emitter, which has greater cytotoxic effects than β^--emitters, the absorbed dose of ^{211}At-MABG was estimated with a radiation weighting factor of 5, as recommended by the MIRD committee [24], and is presented as Sv/MBq in Table 2. The highest absorbed dose was in the stomach (26.8 Sv/MBq), followed by the thyroid (25.0 Sv/MBq), the adrenal glands (24.0 Sv/MBq), and the heart (22.2 Sv/MBq; Table 2).

Body Weight Changes and the MTD of ^{211}At-MABG

The administration of 1.1 and 2.2 MBq of ^{211}At-MABG induced a slight and transient body weight loss during the first several days, but the differences were not statistically significant compared with day 0 (Figure 1). The two groups treated with higher doses of 3.3 and 4.4 MBq showed statistically significant body weight loss as compared with day 0 (3.3 MBq, $P < .05$ at day 3; 4.4 MBq, $P < .01$ at days 3 and 5; Figure 1). The body weights of mice treated with 3.3 MBq recovered thereafter, whereas all five mice administered 4.4 MBq showed more than 20% body weight loss compared with day 0, resulting in humane treatments to all the five (Figure 1). On the basis of these findings, although the real MTD may be in between 3.3 and 4.4 MBq, in the present study, the MTD of ^{211}At-MABG for male ICR mice was considered to be 3.3 MBq, which was used in the following evaluation. The lowest body weight in mice injected with 3.3 MBq was observed at day 5, and the time points of days 5 and 28 were chosen in the following experiments.

Necropsy and Organ Weight

No visible abnormalities were observed at necropsy 5 and 28 days after injection of 3.3 MBq of ^{211}At-MABG, except for changes in the volumes of several organs, such as the liver, spleen, and kidneys. At day 5, the organ weights of the liver ($P < .05$), spleen ($P < .01$), and kidneys ($P < .01$) were significantly lower than those in the PBS-injected control group (Figure 2). Although marked weight loss of the thyroid and adrenal glands was observed, the differences were not statistically significant (Figure 2). At day 28 after the treatment, all of the organs' weight returned to normal, but then the adrenals did not (Figure 2).

Histologic Analysis

No histologic changes induced by 3.3 MBq of ^{211}At-MABG were observed in hematoxylin and eosin–stained sections of all organs at days 5 and 28, except for the bone marrow at day 5 (Figure 3). In the

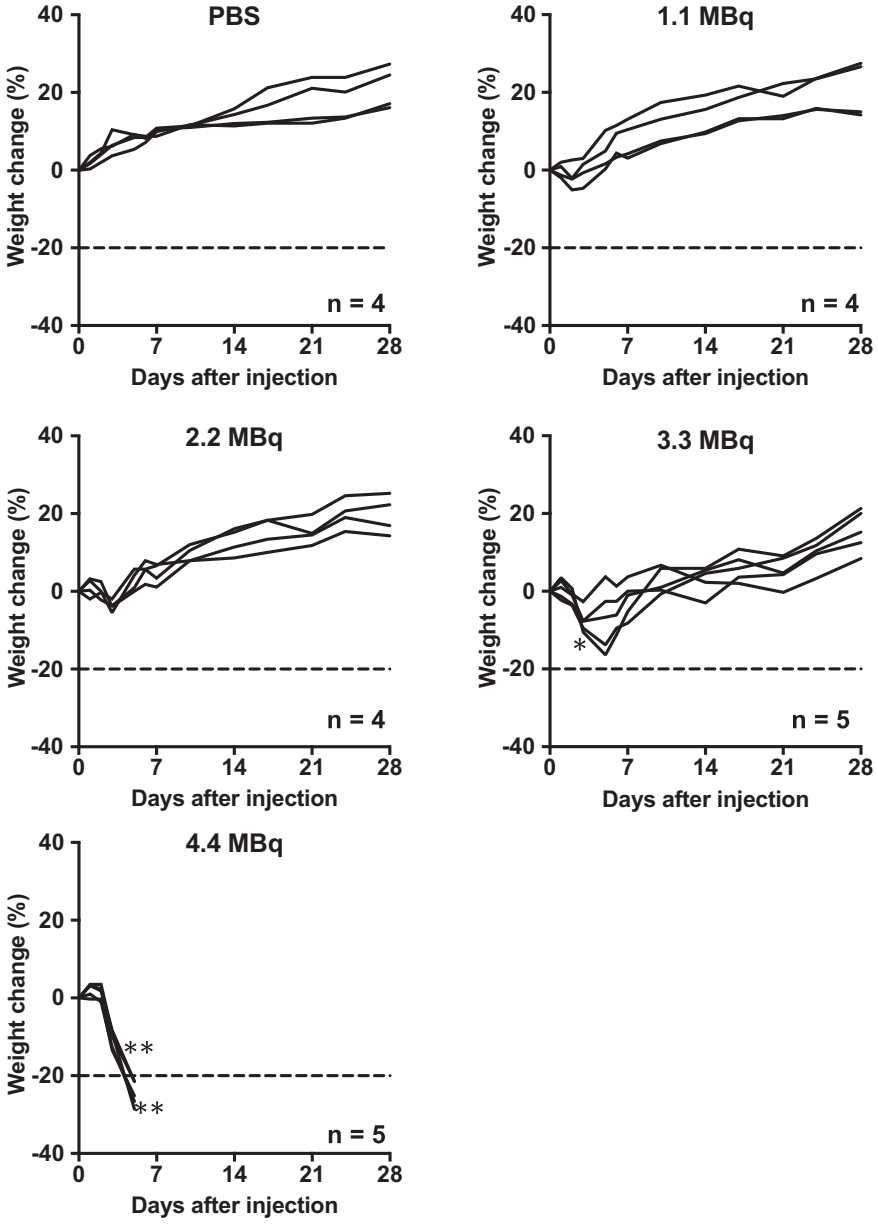

Figure 1. Temporal changes in body weight after administration of PBS ($n = 4$) as a control and ^{211}At-MABG ($n = 4$ or 5 per dose). The dashed line indicates a 20% decrease in body weight relative to day 0. Body weights were compared with those on day 0 and analyzed by repeated-measures one-way analysis of variance with Dunnett's multiple-comparison test.

bone marrow of femurs in the ^{211}At-MABG group, vascular dilation was observed at day 5 but not at day 28 (Figure 3).

Hematologic Parameters

At day 5 after treatment, the number of white blood cells in the ^{211}At-MABG treatment group was significantly lower than that in the control group ($P < .01$, Figure 4). The other hematologic parameters did not significantly differ between the ^{211}At-MABG and control groups at day 5 (Figure 4). At day 28, none of the hematologic parameters differed significantly between the two groups (Figure 4).

Thyroid Hormone and Catecholamine

Although the plasma T3 concentration in the ^{211}At-MABG treatment group was higher than that in the control group at day 5 after administration ($P < .01$), there was no significant difference at day 28 (Figure 5). Similarly, the norepinephrine levels in the ^{211}At-MABG group were significantly higher than those in the control group at day 5 ($P < .05$), whereas there was no significant difference at day 28 (Figure 5). There were no significant differences in the plasma T4 and epinephrine concentrations between the two groups at days 5 and 28 (Figure 5).

Discussion

The α-emitting radiopharmaceutical ^{211}At-MABG is expected to achieve better outcomes in metastatic pheochromocytoma than the β^--emitting radiopharmaceutical ^{131}I-MIBG [11,12,25]. Further clinical studies are required to evaluate the efficacy and toxicity of this radiopharmaceutical in patients [12]. Considering some differences in the biodistribution of radiotracers between animals and humans,

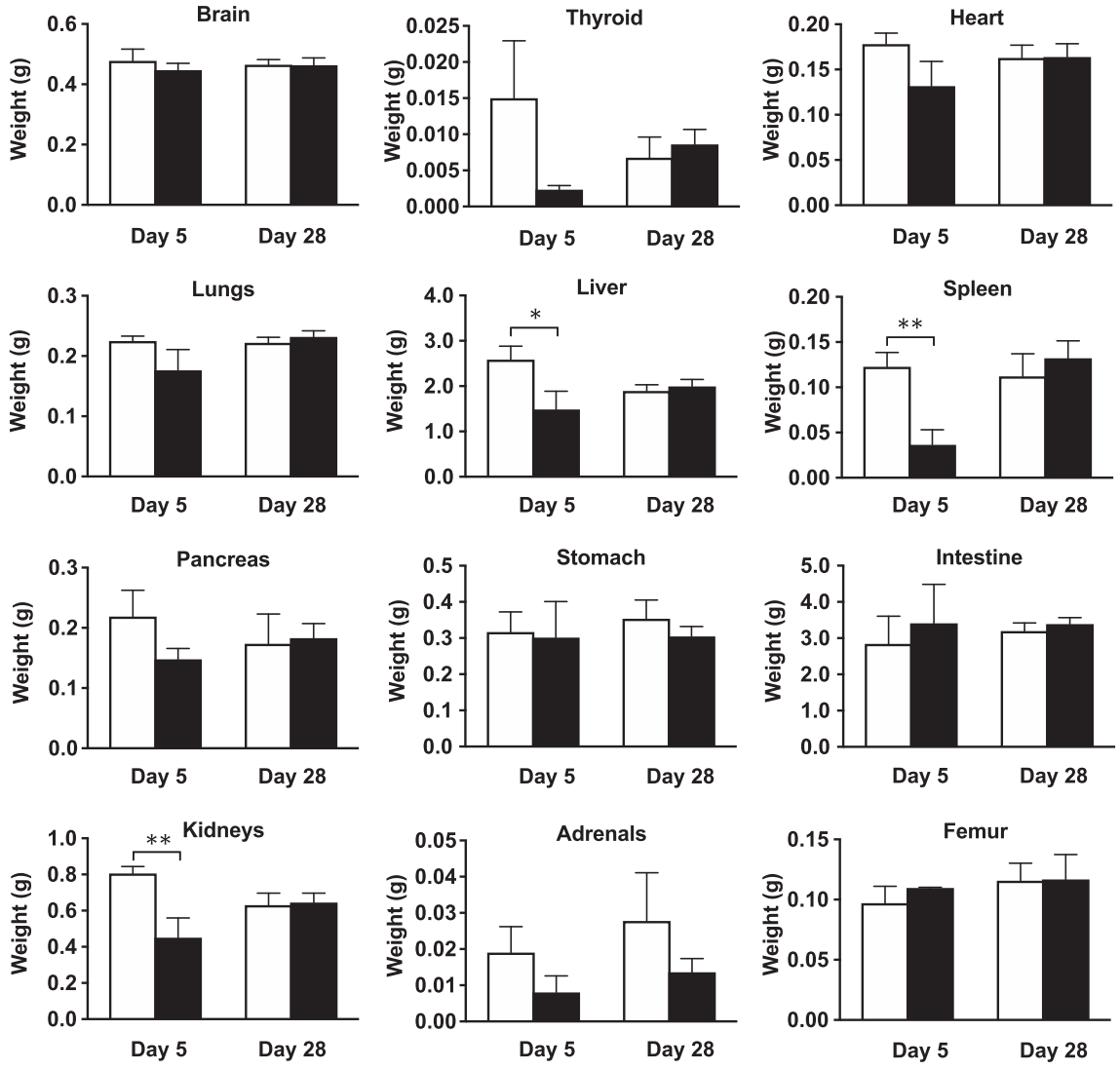

Figure 2. Organ weights at days 5 and 28 after administration of PBS ($n = 3$, open columns) as a control and 3.3 MBq of ^{211}At-MABG ($n = 3$, closed columns) as the MTD. Data indicate mean and standard deviation. $^{**}P < .01$, $^{*}P < .05$ (two-tailed unpaired Student's t test).

including radioiodine-labeled MIBG [14–16], and accumulating clinical experience with ^{131}I-MIBG therapy [6,18], the therapeutic dose of ^{211}At-MABG must be selected according to the biodistribution determined by noninvasive imaging with radioiodine-labeled MIBG (^{123}I-MIBG or ^{131}I-MIBG) in each patient. Generally, radiotoxicity of therapeutic agents is not evaluated in animals before first-in-human studies [13]; however, α-emitting ^{225}Ac-PSMA-617 was recently reported to induce unexpected grade 2 radiation-induced toxicity in two patients [19]. We therefore considered it necessary to evaluate whether ^{211}At-MABG induces unexpected acute radiotoxicity in mice before the first-in-human study is performed. One of our previous studies partially evaluated acute radiation-induced toxicity in nude mice bearing xenografts [12]. Because tumor uptake of ^{211}At-MABG would affect the biodistribution in the whole body, the present study employed non–tumor-bearing ICR mice and included a comprehensive evaluation of acute radiotoxicity.

First, to clarify the absorbed doses of ^{211}At-MABG in each organ, we estimated the dosimetry in ICR mice on the basis of the biodistribution, which was similar to that reported in several previous studies from our laboratory and others [11,12,17]. The absorbed dose was estimated with a radiation weighting factor of 5, as recommended by the MIRD committee, given the relatively higher cytotoxicity of ^{211}At [24]. We observed high absorbed doses in the heart, stomach, adrenal glands, and thyroid. The high doses in the heart and adrenal glands were probably due to high norepinephrine transporter expression [26,27]. In contrast, the high doses in the stomach and thyroid were probably due to high expression of sodium iodide symporters [28]. The carbon-astatine bond is relatively weak, and similarly to iodine, free astatine accumulates in the thyroid and stomach *via* sodium iodide symporters [29]. These findings suggest that administration of high doses of ^{211}At-MABG may provide information on radiotoxicity induced by ^{211}At-MABG.

Next, to determine the MTD of ^{211}At-MABG for ICR mice, we treated the mice with four doses of 1.1, 2.2, 3.3, and 4.4 MBq and measured the temporal changes in body weight. The changes revealed that the dose of 3.3 MBq was the MTD for ICR mice under our experimental conditions. After administration of 3.3 MBq of ^{211}At-MABG, the estimated absorbed doses in the heart, lungs, liver,

spleen, stomach, kidneys, and thyroid were markedly greater than the MTD of radiation: 40 Gy for the heart, 17.5 Gy for the lungs, 30 Gy for the liver, 20 Gy for the spleen, 50 Gy for the stomach, 23 Gy for the kidneys, and 45 Gy for the thyroid [30–33]. The adrenal glands are radioresistant, and irreversible radiation-induced damage has not been reported to date; consequently, the MTD has not been established [34,35]. From our results, we considered the dose of 3.3 MBq sufficient for the purposes of the present study.

Finally, we evaluated the acute radiation-induced toxicity at 3.3 MBq of ^{211}At-MABG according to organ weights, histologic features, hematologic indices, and biochemical indices. There was no visible abnormality at necropsy 5 and 28 days after injection, except for changes in the volumes of several organs, such as the liver, spleen, and kidneys. The effects of radiotoxicity on organ weights, histologic features, hematologic parameters, and hormonal concentration were then evaluated. Although statistically significant weight loss was

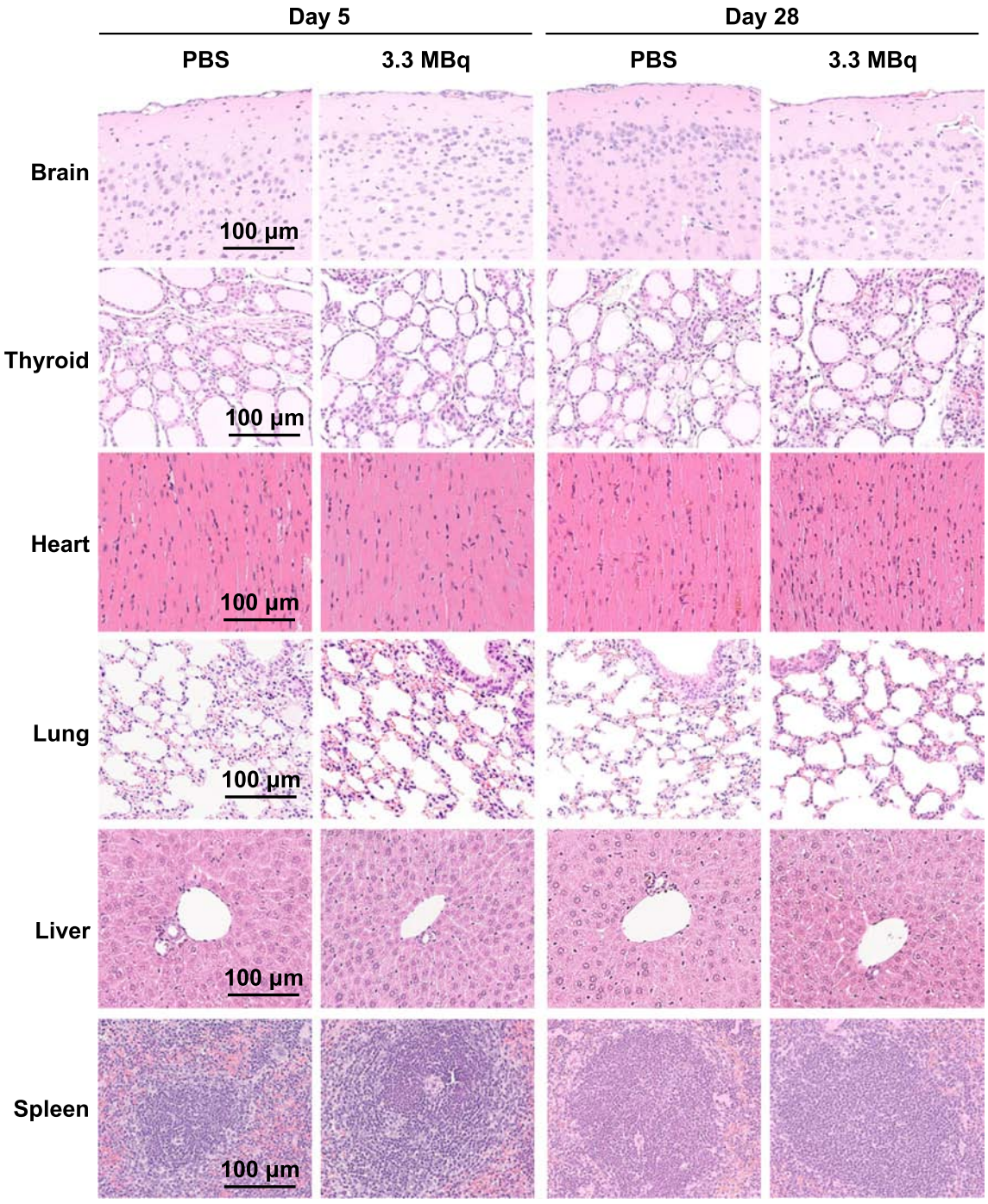

Figure 3. Histologic analysis at days 5 and 28 after administration of 3.3 MBq of ^{211}At-MABG as the MTD or PBS as a control. Representative hematoxylin and eosin–stained sections (1 μm thick) are shown. Black arrows in the bone marrow indicate vascular dilation. Scale bars = 100 μm.

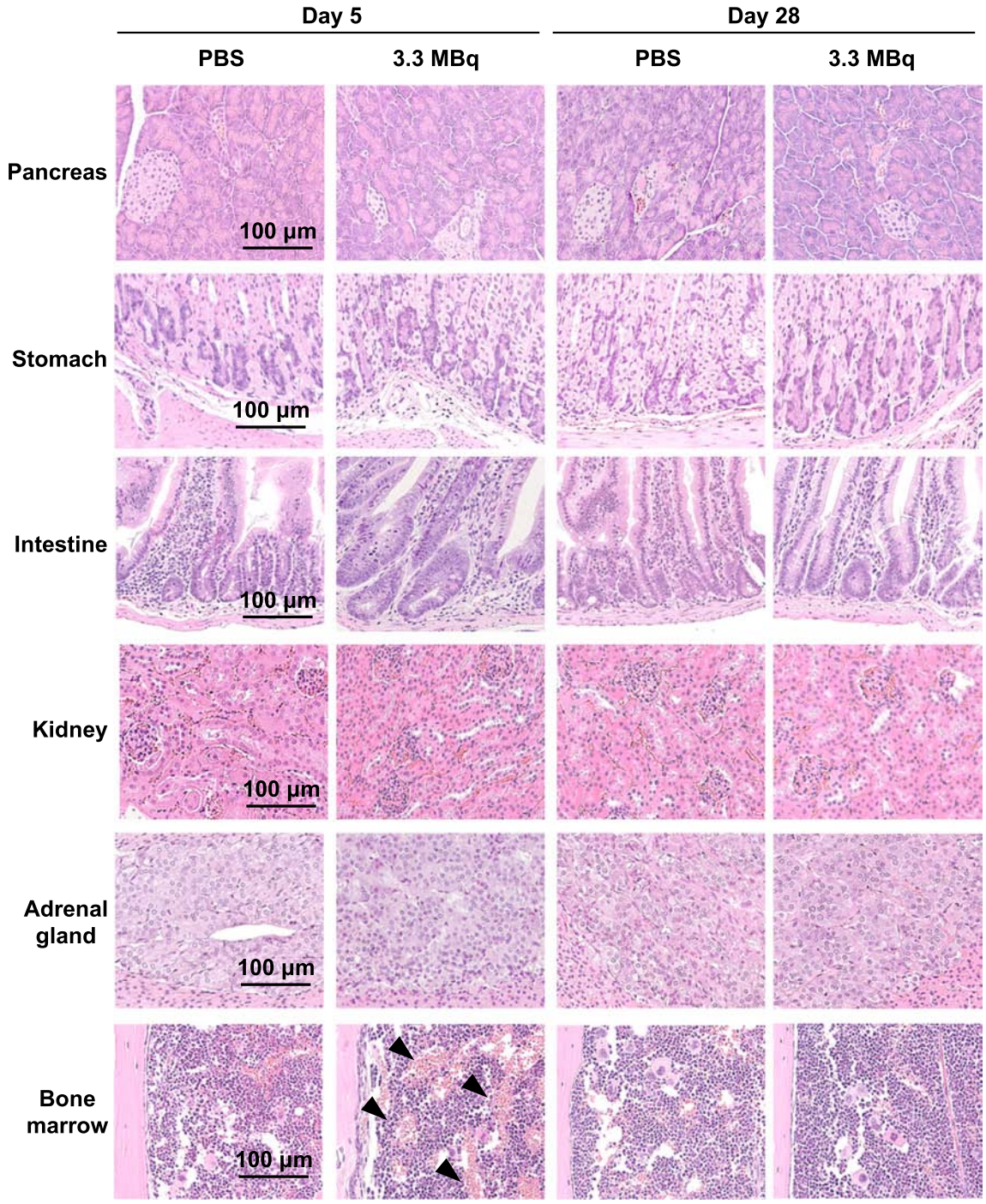

Figure 3 (*continued*).

observed in several organs, such as the liver, spleen, and kidneys, at day 5 after administration, there was no significant difference at day 28 relative to the control group. No significant histologic changes in those organs showing significant weight loss were observed at days 5 and 28. The bone marrow showed vascular dilation at day 5 but not at day 28. This abnormal feature was also observed in nude mice bearing tumors [12]. In addition, a lower number of white blood cells were observed at day 5 but not at day 28. These reversible adverse effects are usually observed in radiation therapy including therapy with ^{131}I-MIBG [18]. Moreover, after treatment with another α-emitting therapeutic agent, ^{225}Ac-PSMA-617, some patients show reversible hematologic toxicity symptoms such as thrombocytopenia, neutropenia, and leucopenia [19]. In the present study, we observed marked weight loss in the thyroid and adrenal glands, but the results were not statistically significant; in addition, there were no histologic changes. Nonetheless, transient increases in T3 and norepinephrine in these organs are reported [36,37]. The present study used no blocking agent, such as potassium iodide, to evaluate maximum radiation-induced toxicity; however, the use of appropriate blocking agents has enabled decreased radiation doses in the thyroid and stomach in clinical studies [38]. Our findings suggest that ^{211}At-MABG treatment would be well tolerated and have a low risk of unexpected

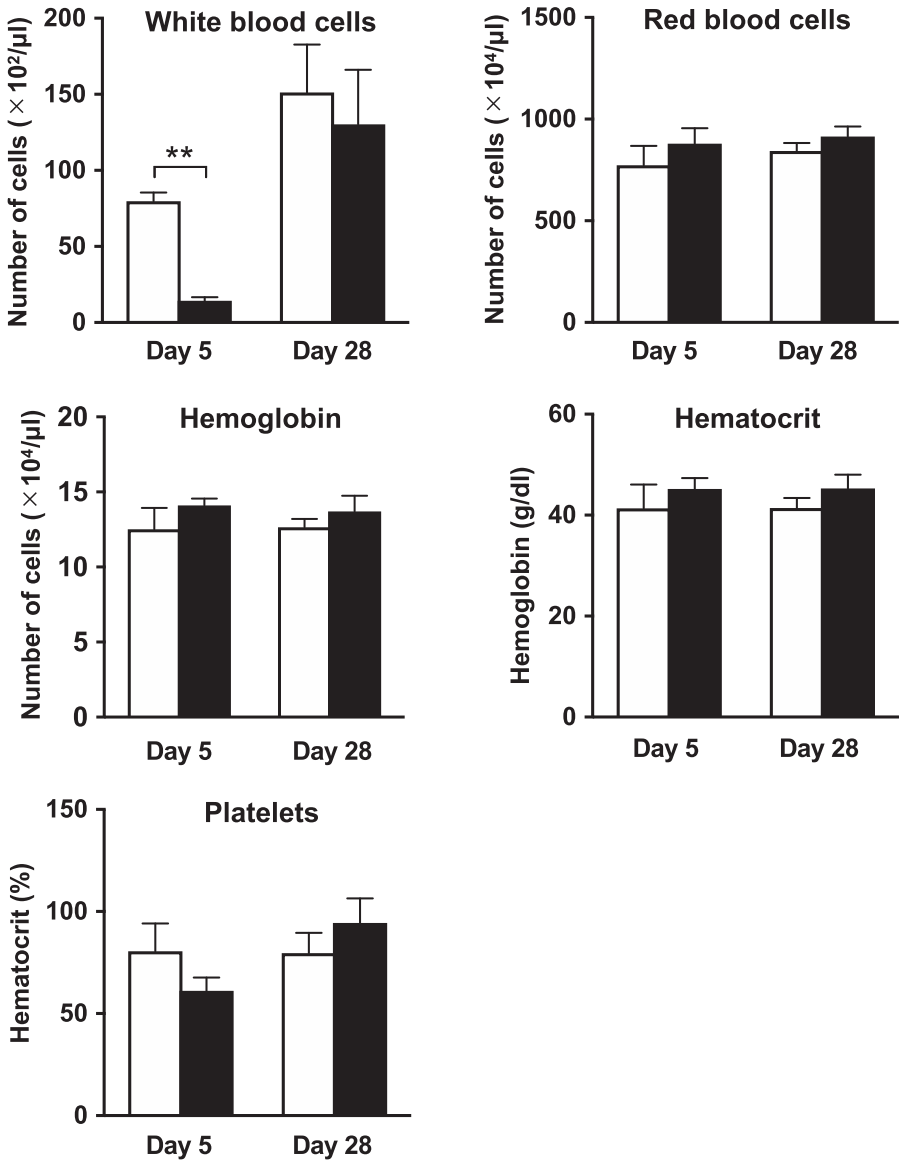

Figure 4. Hematologic analysis at days 5 and 28 after administration of PBS ($n = 3$, open columns) as a control or 3.3 MBq of ^{211}At-MABG ($n = 3$, closed columns) as the MTD. Data indicate mean and standard deviation. $^{**}P < .01$ (two-tailed unpaired Student's t test).

acute radiation-related toxicity. Therefore, dosimetry studies in patients would be appropriate for selecting the therapeutic doses of ^{211}At-MABG in clinical studies, although lower doses may be required initially to ensure safety.

Although the present study showed that high doses of ^{211}At-MABG were well tolerated in mice and unexpected radiation-induced toxicity was not observed under our conditions, the study has several limitations. First, because a small number of mice were used to evaluate acute radiotoxicity, we cannot completely exclude the possibility that some toxicity induced by ^{211}At-MABG might have been missed. Second, the present examination in male mice cannot address the possibility that some toxicity might be present only in females, although to our knowledge, no female-specific toxicity has been reported in patients treated with ^{131}I-MIBG. The first-in-human study could be conducted in male patients to avoid such risks. Third, no long-term toxicity assessments were included in the present study. Irreversible late radiation toxicity in the kidneys and bladder has been reported in clinical trials with two radiopharmaceuticals, even though the injected doses were limited on the basis of general knowledge of radiation toxicity [39,40]. The FDA recommends long-term toxicity assessment when patients have a long life expectancy that could be affected by late adverse effects of radiation [13]. After the therapeutic effects of ^{211}At-MABG are established in patients, evaluation of late radiation toxicity might be required.

In conclusion, our biodistribution and dosimetry studies revealed that α-emitting ^{211}At-MABG delivered high radiation doses to most organs except the brain in ICR mice. The administration of 3.3 MBq, the MTD for ICR mice, induced transient radiation-related toxicity symptoms that recovered at day 28 and are generally observed in radiation therapy including β^--emitting ^{131}I-MIBG. Unexpected severe toxicity was not observed in the present study, although high radiation doses were absorbed by most organs, especially the thyroid, heart, stomach, and adrenal glands, after injection of 3.3 MBq of ^{211}At-MABG. Our findings suggest that therapeutic treatment with

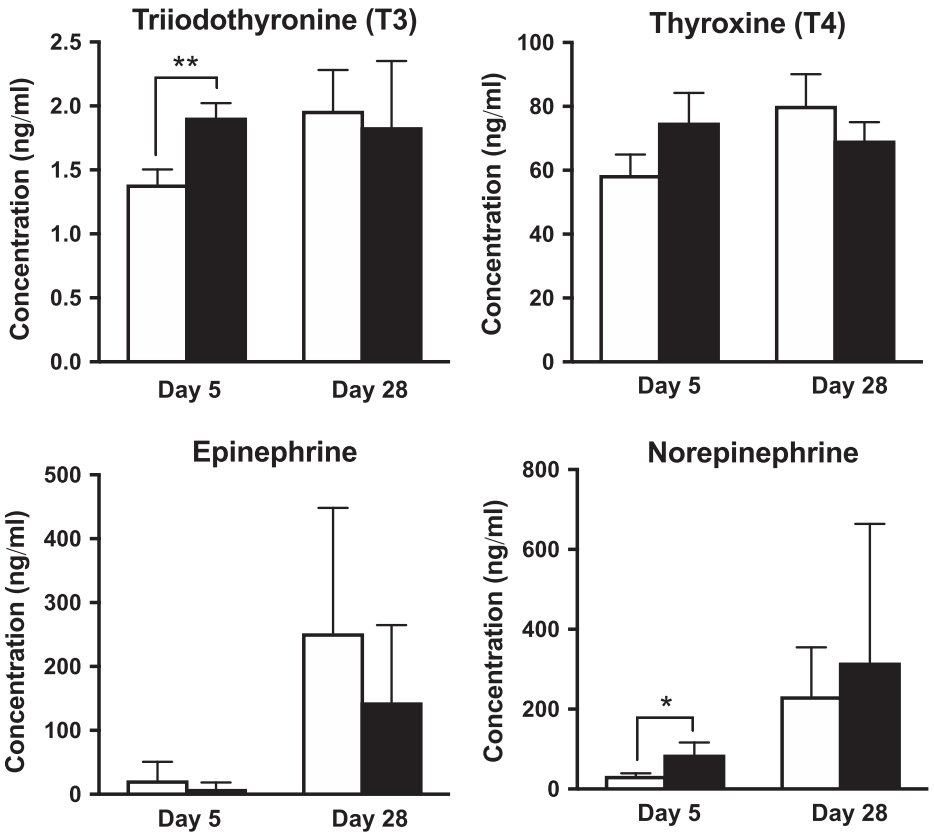

Figure 5. Concentrations of hormones (T3, T4, epinephrine, and norepinephrine) in the plasma at days 5 and 28 after administration of PBS (n = 3, open columns) as a control or 3.3 MBq of ^{211}At-MABG (n = 3, closed columns) as the MTD. Data indicate mean and standard deviation. $^{**}P < .01$, $^{*}P < .05$ (two-tailed unpaired Student's t test).

appropriate doses of ^{211}At-MABG estimated by dosimetry in each patient could be tolerated, although there may be a need to start with lower doses to ensure safety in the first-in-human study.

Acknowledgement

We thank Yuriko Ogawa and Naoko Kuroda for technical assistance for animal experiments and the staff in the Laboratory Animal Sciences section for animal management.

Disclosure

The authors declare no conflict of interest.

References

[1] Lenders JW, Eisenhofer G, Mannelli M, and Pacak K (2005). Phaeochromocytoma. *Lancet* **366**, 665–675.

[2] Ayala-Ramirez M, Feng L, Johnson MM, Ejaz S, Habra MA, Rich T, Busaidy N, Cote GJ, Perrier N, and Phan A, et al (2011). Clinical risk factors for malignancy and overall survival in patients with pheochromocytomas and sympathetic paragangliomas: primary tumor size and primary tumor location as prognostic indicators. *J Clin Endocrinol Metab* **96**, 717–725.

[3] Lenders JW, Duh QY, Eisenhofer G, Gimenez-Roqueplo AP, Grebe SK, Murad MH, Naruse M, Pacak K, and Young Jr WF (2014). Pheochromocytoma and paraganglioma: an endocrine society clinical practice guideline. *J Clin Endocrinol Metab* **99**, 1915–1942.

[4] Yoshinaga K, Oriuchi N, Wakabayashi H, Tomiyama Y, Jinguji M, Higuchi T, Kayano D, Fukuoka M, Inaki A, and Toratani A, et al (2014). Effects and safety of ^{131}I-metaiodobenzylguanidine (MIBG) radiotherapy in malignant neuroendocrine tumors: results from a multicenter observational registry. *Endocr J* **61**, 1171–1180.

[5] Young Jr WF (2010). Endocrine hypertension: then and now. *Endocr Pract* **16**, 888–902.

[6] van Hulsteijn LT, Niemeijer ND, Dekkers OM, and Corssmit EP (2014). ^{131}I-MIBG therapy for malignant paraganglioma and phaeochromocytoma: systematic review and meta-analysis. *Clin Endocrinol (Oxf)* **80**, 487–501.

[7] Tanabe A, Naruse M, Nomura K, Tsuiki M, Tsumagari A, and Ichihara A (2013). Combination chemotherapy with cyclophosphamide, vincristine, and dacarbazine in patients with malignant pheochromocytoma and paraganglioma. *Horm Cancer* **4**, 103–110.

[8] Pheochromocytoma and Paraganglioma Treatment (PDQ(R)): Health Professional VersionPDQ Cancer Information Summaries. Bethesda, MD, USA: National Cancer Institute; 2002 .

[9] Gonias S, Goldsby R, Matthay KK, Hawkins R, Price D, Huberty J, Damon L, Linker C, Sznewajs A, and Shiboski S, et al (2009). Phase II study of high-dose [^{131}I] metaiodobenzylguanidine therapy for patients with metastatic pheochromocytoma and paraganglioma. *J Clin Oncol* **27**, 4162–4168.

[10] Baidoo KE, Yong K, and Brechbiel MW (2013). Molecular pathways: targeted alpha-particle radiation therapy. *Clin Cancer Res* **19**, 530–537.

[11] Vaidyanathan G and Zalutsky MR (1992). 1-(m-[^{211}At]astatobenzyl)guanidine: synthesis via astato demetalation and preliminary in vitro and in vivo evaluation. *Bioconjug Chem* **3**, 499–503.

[12] Ohshima Y, Sudo H, Watanabe S, Nagatsu K, Tsuji AB, Sakashita T, Ito YM, Yoshinaga K, Higashi T, and Ishioka NS (2018). Antitumor effects of radionuclide treatment using alpha-emitting meta-^{211}At-astato-benzylguanidine in a PC12 pheochromocytoma model. *Eur J Nucl Med Mol Imaging* **45**, 999–1010.

[13] Food and Drug Administration (2018). Oncology therapeutic radiopharmaceuticals: nonclinical studies and labeling recommendations, guidance for Industry; 2018.

[14] Giammarile F, Chiti A, Lassmann M, Brans B, and Flux G (2008). Eanm. EANM procedure guidelines for ^{131}I-meta-iodobenzylguanidine (^{131}I-mIBG) therapy. *Eur J Nucl Med Mol Imaging* **35**, 1039–1047.

[15] Vaidyanathan G, Friedman HS, Keir ST, and Zalutsky MR (1996). Localisation of [^{131}I]MIBG in nude mice bearing SK-N-SH human neuroblastoma xenografts: effect of specific activity. *Br J Cancer* **73**, 1171–1177.

[16] Ko BH, Paik JY, Jung KH, Bae JS, Lee EJ, Choe YS, Kim BT, and Lee KH (2008). Effects of anesthetic agents on cellular ^{123}I-MIBG transport and in vivo ^{123}I-MIBG biodistribution. *Eur J Nucl Med Mol Imaging* **35**, 554–561.

[17] Vaidyanathan G, Friedman HS, Keir ST, and Zalutsky MR (1996). Evaluation of meta-[^{211}At]astatobenzylguanidine in an athymic mouse human neuroblastoma xenograft model. *Nucl Med Biol* **23**, 851–856.

[18] Kayano D and Kinuya S (2018). Current consensus on I-131 MIBG therapy. *Nucl Med Mol Imaging* **52**, 254–265.

[19] Kratochwil C, Bruchertseifer F, Rathke H, Bronzel M, Apostolidis C, Weichert W, Haberkorn U, Giesel FL, and Morgenstern A (2017). Targeted alpha-therapy of metastatic castration-resistant prostate cancer with (225)Ac-PSMA-617: dosimetry estimate and empiric dose finding. *J Nucl Med* **58**, 1624–1631.

[20] Nagatsu K, Minegishi K, Fukada M, Suzuki H, Hasegawa S, and Zhang MR (2014). Production of ^{211}At by a vertical beam irradiation method. *Appl Radiat Isot* **94**, 363–371.

[21] Yoshida C, Tsuji AB, Sudo H, Sugyo A, Kikuchi T, Koizumi M, Arano Y, and Saga T (2013). Therapeutic efficacy of c-kit-targeted radioimmunotherapy using ^{90}Y-labeled anti-c-kit antibodies in a mouse model of small cell lung cancer. *PLoS One* **8**e59248.

[22] Li HK, Sugyo A, Tsuji AB, Morokoshi Y, Minegishi K, Nagatsu K, Kanda H, Harada Y, Nagayama S, and Katagiri T, et al (2018). alpha-particle therapy for synovial sarcoma in the mouse using an astatine-211-labeled antibody against frizzled homolog 10. *Cancer Sci* **109**, 2302–2309.

[23] Eckerman KF and Endo A (2008). MIRD: Radionuclide Data and Decay Schemes. 2nd ed. Reston, VA: The Society of Nuclear Medicine and Molecular Imaging; 2008.

[24] Sgouros G, Roeske JC, McDevitt MR, Palm S, Allen BJ, Fisher DR, Brill AB, Song H, Howell RW, and Akabani G, et al (2010). MIRD Pamphlet No. 22 (abridged): radiobiology and dosimetry of alpha-particle emitters for targeted radionuclide therapy. *J Nucl Med* **51**, 311–328.

[25] Strickland DK, Vaidyanathan G, and Zalutsky MR (1994). Cytotoxicity of alpha-particle-emitting m-[^{211}At]astatobenzylguanidine on human neuroblastoma cells. *Cancer Res* **54**, 5414–5419.

[26] Li H, Ma SK, Hu XP, Zhang GY, and Fei J (2001). Norepinephrine transporter (NET) is expressed in cardiac sympathetic ganglia of adult rat. *Cell Res* **11**, 317–320.

[27] Pandit-Taskar N and Modak S (2017). Norepinephrine transporter as a target for imaging and therapy. *J Nucl Med* **58**, 39S–53S.

[28] Hingorani M, Spitzweg C, Vassaux G, Newbold K, Melcher A, Pandha H, Vile R, and Harrington K (2010). The biology of the sodium iodide symporter and its potential for targeted gene delivery. *Curr Cancer Drug Targets* **10**, 242–267.

[29] Poty S, Francesconi LC, McDevitt MR, Morris MJ, and Lewis JS (2018). alpha-Emitters for radiotherapy: from basic radiochemistry to clinical studies—part 1. *J Nucl Med* **59**, 878–884.

[30] Emami B, Lyman J, Brown A, Coia L, Goitein M, Munzenrider JE, Shank B, Solin LJ, and Wesson M (1991). Tolerance of normal tissue to therapeutic irradiation. *Int J Radiat Oncol* **21**, 109–122.

[31] Burman C, Kutcher GJ, Emami B, and Goitein M (1991). Fitting of normal tissue tolerance data to an analytic function. *Int J Radiat Oncol Biol Phys* **21**, 123–135.

[32] Weinmann M, Becker G, Einsele H, and Bamberg M (2001). Clinical indications and biological mechanisms of splenic irradiation in chronic leukaemias and myeloproliferative disorders. *Radiother Oncol* **58**, 235–246.

[33] Meredith R, Wessels B, and Knox S (2008). Risks to normal tissues from radionuclide therapy. *Semin Nucl Med* **38**, 347–357.

[34] Rosol TJ, Yarrington JT, Latendresse J, and Capen CC (2001). Adrenal gland: structure, function, and mechanisms of toxicity. *Toxicol Pathol* **29**, 41–48.

[35] Fajardo LF, Berthrong M, and Anderson RE (2001). Radiation Pathology. New York, NY, USA: Oxford University Press; 2001.

[36] Carvalho DP and Dupuy C (2017). Thyroid hormone biosynthesis and release. *Mol Cell Endocrinol* **458**, 6–15.

[37] Perlman RL and Chalfie M (1977). Catecholamine release from the adrenal medulla. *Clin Endocrinol Metab* **6**, 551–576.

[38] Larsen RH, Slade S, and Zalutsky MR (1998). Blocking [211At]astatide accumulation in normal tissues: preliminary evaluation of seven potential compounds. *Nucl Med Biol* **25**, 351–357.

[39] Giralt S, Bensinger W, Goodman M, Podoloff D, Eary J, Wendt R, Alexanian R, Weber D, Maloney D, and Holmberg L, et al (2003). ^{166}Ho-DOTMP plus melphalan followed by peripheral blood stem cell transplantation in patients with multiple myeloma: results of two phase 1/2 trials. *Blood* **102**, 2684–2691.

[40] Moll S, Nickeleit V, Mueller-Brand J, Brunner FP, Maecke HR, and Mihatsch MJ (2001). A new cause of renal thrombotic microangiopathy: yttrium 90-DOTATOC internal radiotherapy. *Am J Kidney Dis* **37**, 847–851.